JOURNAL OF AIRCRAFT
Vol. 38, No. 6, November–December 2001

Design-Oriented High-Lift Methodology for General Aviation and Civil Transport Aircraft

C. P. van Dam,* J. C. Vander Kam,† and J. K. Paris‡
University of California—Davis, Davis, California 95616-5294

A high-lift system design methodology that can be incorporated during the early stages of aircraft development is presented and thus has the potential to provide a superior and more cost-effective vehicle than one developed utilizing traditional linear design methods. The present methodology offers two different levels of fidelity: one applicable to the conceptual design stage and the other to the preliminary design stage. The underlying flow solver couples a three-dimensional nonlinear Weissinger method with two-dimensional viscous data to provide fast and accurate aerodynamic predictions for high-lift configurations. Several test cases that illustrate the capabilities of this hybrid flow solver are presented.

Nomenclature

AR	=	aspect ratio, b^2/S
b	=	wing span
C_L	=	lift coefficient
C_l	=	sectional lift coefficient
$C_{l_{\text{visc}}}$	=	sectional lift coefficient based on viscous analysis (see Fig. 8)
C_{l_W}	=	sectional lift coefficient based on inviscid analysis (see Fig. 8)
C_{l_α}	=	sectional lift curve slope
c	=	local chord length
c_f	=	flap chord length
M_∞	=	freestream Mach number
Re	=	reynolds number based on freestream conditions and reference chord
S	=	wing reference area
x	=	chord location
$xtran$	=	chordwise boundary-layer transition location
y	=	semispan location
α	=	angle of attack
α_{local}	=	sectional angle of attack
α_0	=	sectional angle of attack for zero lift
$\Delta\alpha_{\text{visc}}$	=	change in sectional angle of attack as a result of viscous effects (see Fig. 8)
δ_f	=	flap deflection angle
ε	=	allowable error
η	=	nondimensional semispan station, $y/(b/2)$
χ	=	flap flow separation factor

Introduction

ALTHOUGH the design methods and tools used in commercial aircraft development have changed over the years, the overall goal of aircraft production has remained the same: to provide the customer with a cost-effective, high-quality product that meets a desired set of mission requirements.

In the highly competitive and economically driven commercial aviation market of today, the trend is to make aircraft systems simpler, which results in lower production and operational costs. One such system is the high-lift system. An aircraft's high-lift system is vital for the takeoff and landing stages of flight and accounts for somewhere between 6 and 11% (potentially higher for more complex configurations) of the production cost of a typical jet transport.[1]

It is important to understand the significant impact that the early stages of design have on the overall complexity and cost of the resulting high-lift system. As outlined by Nield,[2] aircraft have traditionally been designed in a sequential fashion, leaving the high-lift design to near the end when much of the aircraft geometry has already been committed. This approach is illustrated in Fig. 1. In a typical product development program 90% of the cost is committed in the first 10% of the design cycle.[3] Addressing design of the high-lift system earlier in the aircraft design cycle can make it possible to utilize a simpler high-lift system, which would significantly reduce aircraft production cost. Additionally, the ability to evaluate high-lift system considerations early on in the design process makes it possible to design for growth of the high-lift system for derivative aircraft or to simply avoid problems later in the design process, for example, finding out after the configuration freeze that the required $C_{L_{\max}}$ calls for an high-lift system whose mechanisms do not fit in the allotted space.

This paper presents a methodology for incorporating high-lift system design considerations in the early stages of an aircraft development cycle. The goals of this continuing effort are to design and develop a high-lift methodology that 1) encompasses all critical design elements, 2) is fast and accurate, 3) is fully scalable with respect to hardware, software, and high-lift technology advancements, and 4) can be applied early on in the airplane development process.

A high-lift system design code, referred to as the *high-lift module*, was developed as a "plug-in" module for an existing aircraft conceptual design package called the AirCraft SYNThesis (ACSYNT) program.[4] ACSYNT, developed by the Systems Analysis Branch at NASA Ames Research Center, allows an aircraft designer to perform tradeoff studies, sensitivities, and optimizations of various aircraft configurations. Analysis modules include aerodynamics, weights, propulsion, mission performance, geometry, stability and control, economics, and the newly developed high-lift module. The present work is an extension of the work by Pepper et al.[5] and Pepper and van Dam[6] offering a methodology for the conceptual design of high-lift systems including cost, weight, and aerodynamic prediction methods for multielement high-lift configurations. Recently the method was modified to allow for more flexibility in terms of wing geometry, to include the aerodynamics of main/aft double-slotted flaps, and to provide a methodology capable of producing higher-fidelity aerodynamic predictions, including maximum lift coefficient, for

Received 31 July 2000; revision received 1 July 2001; accepted for publication 24 July 2001.

*Professor, Department of Mechanical and Aeronautical Engineering, One Shields Avenue; cpvandam@ucdavis.edu.

†Graduate Research Assistant, Department of Mechanical and Aeronautical Engineering, One Shields Avenue; currently Research Scientist, Eloret, Inc./NASA Ames Research Center, Moffet Field, CA; jvanderkam@mail.arc.nasa.gov.

‡Graduate Research Assistant, Department of Mechanical and Aeronautical Engineering; currently Engineer/Scientist, The Boeing Company; john.k.paris@boeing.com.

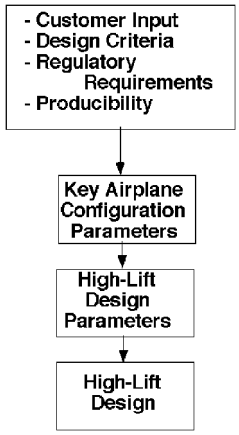

Fig. 1 High-lift design methodology—traditional approach.[2]

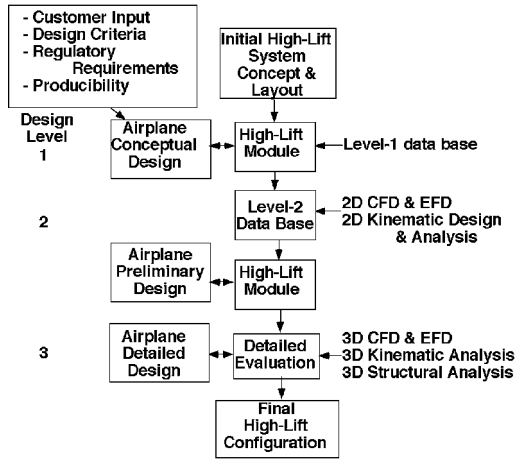

Fig. 2 High-lift design methodology—improved approach.

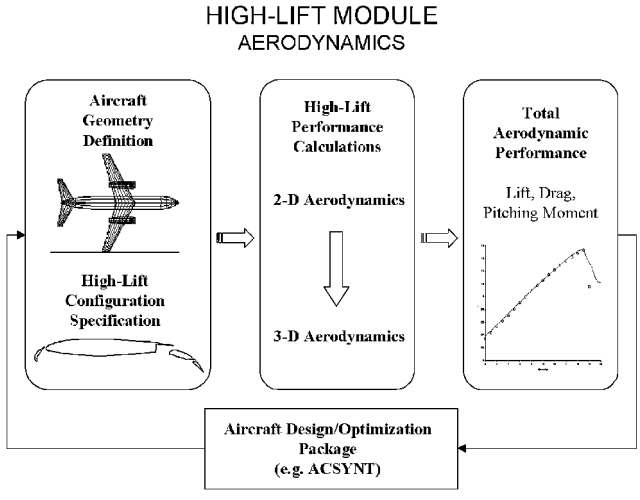

Fig. 3 Overview of the high-lift module aerodynamic analysis.

use at the preliminary design stage. Not only does this paper build upon previous high-lift research, it also complements the efforts by van Dam et al.,[7,8] who developed an aeromechanical design methodology for high-lift deployment systems.

The proposed high-lift design methodology is presented in Fig. 2. Note that it integrates critical high-lift design elements into the early stages of the aircraft design process. One of the key components of this proposed approach is the high-lift module. The high-lift module provides the necessary high-lift system cost, weight, and aerodynamic performance predictions utilized at the conceptual and preliminary stages of an aircraft design. This paper focuses on the aerodynamic portion of the high-lift module, which is depicted in Fig. 3. To utilize the high-lift module at the conceptual and preliminary design stages of an aircraft design, it is essential that the aerodynamic predictions be made quickly. For this reason a fast lifting-line method (modified Weissinger method) closely coupled with two-dimensional viscous data is utilized to calculate the three-dimensional aerodynamic characteristics. The result is a high-lift module that has a good balance between speed and accuracy, making it an effective tool for use at the early stages of aircraft design.

Two-Dimensional Aerodynamic Modeling

The sectional aerodynamic characteristics are a key ingredient to the three-dimensional aerodynamic analysis as illustrated in Fig. 3. The high-lift module determines the two-dimensional aerodynamic characteristics of each airfoil section in one of two ways. One option is to utilize the two-dimensional semi-empirical equations, which are based on computational fluid dynamics (CFD) and experimental data for various modern high-lift configurations (level 1 aerodynamic database; see Fig. 2). Because this method does not require a detailed description of the airfoil geometry but rather a parametric representation of the configuration, it is most applicable at the conceptual design stage of an aircraft. Once at the preliminary design stage, typically more detailed geometric and aerodynamic information is available. At this point higher fidelity two-dimensional aerodynamic data (level 2 database; see Fig. 2) can be imported directly into the high-lift module.

There are two ways to acquire the two-dimensional aerodynamic performance results for the level 2 database: experimentally through two-dimensional high-lift wind-tunnel tests for a wide range of relevant configurations or computationally using numerical simulation methods. Given the current fiscal climate, it is very difficult to conduct extensive experimental high-lift research programs such as those conducted in the United States in the 1940s and the United Kingdom in the 1970s.[9,10] Fortunately, computer technology and algorithms for solving complex flow problems have improved rapidly in the recent years, making CFD an efficient and cost-effective method of analyzing high-lift airfoils. Although a good deal of experimental data exists for a variety of high-lift systems, most of it is at low Reynolds numbers and is based on out-dated high-lift configurations. Therefore, CFD provides the necessary and cost-effective means of acquiring two-dimensional high-lift data of modern high-lift configurations at flight Reynolds numbers.

A well-validated incompressible Reynolds-averaged Navier–Stokes solver called INS2D[11] was selected for the two-dimensional CFD analysis. This code has been validated as an accurate tool in the simulation of viscous flow over multielement airfoils at high Reynolds numbers.[12,13] In addition, the code's ability to accurately predict trends caused by geometric changes of high-lift airfoils has been verified in a design optimization environment by Eyi et al.[14] Van Dam et al.[7,8] also show that the trends in lift and drag caused by changes in trailing-edge flap gap and overlap predicted by INS2D correspond very well with experiment. Although there are other computational tools available for the analysis of high-lift systems, INS2D was chosen because of its proven accuracy and reliability and also because the tools for pre- and postprocessing of INS2D simulations are readily available at University of California—Davis. A disadvantage of this incompressible flow solver is that it does not capture Mach-number effects on airfoil maximum lift characteristics.

The Spalart–Allmaras[15] turbulence model was used, which solves one transport equation for a nondimensional eddy viscosity variable. This model, unlike many other turbulence models, provides a smooth laminar to turbulent transition at points specified by the user. This "ramping" effect from laminar to turbulent flow can be troublesome at times when precise control of the transition point is desired. Nonetheless, this model in conjunction with INS2D has been shown to produce results that compare very well with experimental multielement aerodynamic data.

Of particular interest to high-lift design, the Spalart–Allmaras turbulence model seems to be the best in predicting sectional stall angle and maximum lift coefficient $C_{l_{\max}}$, as shown by Rogers et al.[16] in their evaluation of four different turbulence models available in INS2D. Similar results demonstrating the excellent $C_{l_{\max}}$ predictive capabilities of INS2D using the Spalart–Allmaras turbulence model

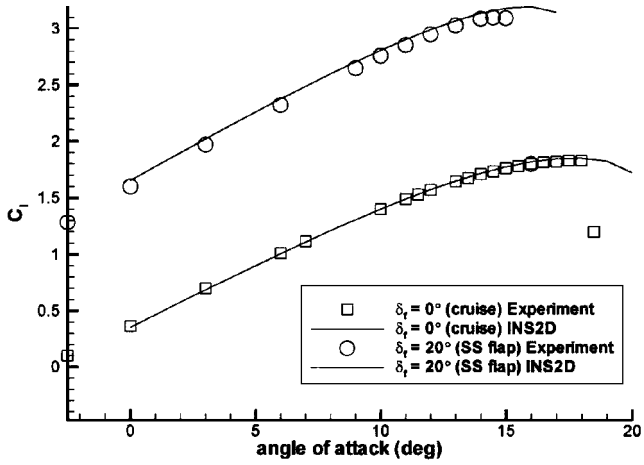

Fig. 4 Comparison of measured and predicted (INS2D) lift curves for a modern civil transport aircraft airfoil in cruise configuration and with a single-slotted Fowler flap in takeoff position, $Re = 6.9 \times 10^6$, $xtran_{upper} = 0.02c$, $xtran_{lower} = 0.20c$, flap fully turbulent.

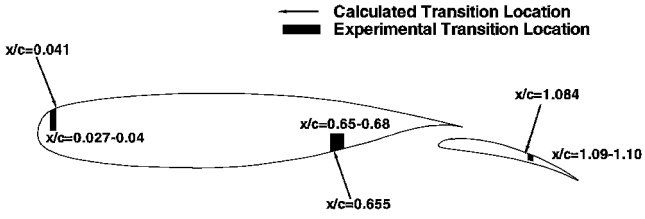

Fig. 5 Measured and predicted transition locations for the NLR-7301 flapped airfoil, $\alpha = 6$ deg, $\delta_f = 20$ deg, $Re = 2.51 \times 10^6$, flap gap = $0.026c$, flap overlap = $0.053c$.

are shown in Fig. 4. The airfoils (cruise and single-slotted flap) analyzed were rotated to 10-deg angle of attack, and then the grids were generated. This allowed the flow physics in the wake to be captured more accurately at higher angles of attack, which experience has shown to be an important factor in accurate $C_{l_{max}}$ predictions.

Because of the sensitivity of high-lift aerodynamics to boundary-layer transition, some attention must be paid to transition location on the airfoil elements. Recently, a transition prediction algorithm has been incorporated into the INS2D flow solver that makes it possible to determine the onset of transition automatically as the flow solution converges. This methodology identifies several transition mechanisms. In two-dimensional airfoil flows, where surfaces are generally smooth and freestream turbulence levels are low, transition is governed by Tollmien–Schlichting (TS) instability, laminar separation, or turbulence contamination.[17] The latter mechanism is often overlooked, but can be important when, for instance, the flap boundary layer is contaminated by the wake of the main element and/or the slat.[18] The method is described in more detail by Brodeur and van Dam.[19] The Navier–Stokes flow solver including the transition prediction formulation has been applied to the NLR 7301 flapped airfoil. The test was conducted for the airfoil with a flap angle of 20 deg, flap gap of 0.026c, and flap overlap of 0.053c at a chord Reynolds number of 2.51×10^6 and an angle of attack of 6 deg. This particular multielement airfoil was selected because of the extensive experimental data available, which include transition measurements.[20] The predicted transition locations are compared to the experimentally observed locations in Fig. 5. On the lower surface of the main element transition is calculated within the range observed in the experiment, whereas transition on the upper surface is predicted slightly aft of the observed range. Transition on the upper surface of the flap is predicted slightly ahead of that seen in the experiment. On the lower surface of the flap, the flow is predicted to remain laminar as in the experiment. In general, the calculated transition points agree well with the experimental observations.

Level 1 Aerodynamic Database

As mentioned earlier, historically the task of high-lift system design has been conducted during the latter stages of the design process after which much of the aircraft geometry has already been frozen. This less-than-optimal approach is a result of the high level of complexity associated with high-lift system design and the lack of efficient and accurate prediction methods that can be used at the conceptual design stage. Critical elements that must be considered in the design of a high-lift system include aerodynamics, cost, weight, mechanics, and noise. The daunting task alone of determining the two-dimensional aerodynamic performance of high-lift systems includes challenges such as confluent shear layers, massive separation, and inverse Reynolds-number effects. Typically, computational methods based on the Reynolds-averaged Navier–Stokes equations are required to capture accurately complex flow physics such as these. Given the current state of computing technology, it is still not practical to utilize Navier–Stokes CFD codes at the conceptual design stage because the solutions tend to take too much time. For this reason semi-empirical methods such as those found in DATCOM[21] remain widely used, but these methods are not sufficiently accurate for the design of a modern civil transport aircraft because they are often based on low-Reynolds-number data and outdated high-lift system technology. One example of this is given in Fig. 6, which presents the empirical flow separation factor χ as a function of flap deflection angle for the two-element flap system on the Energy Efficient Transport (EET).[22] The factor χ is used in the calculation of flap lift effectiveness to account for strong viscous effects and separation in flap flows. One set of curves is obtained from DATCOM, whereas the second set of curves is obtained from computational analysis. Figure 6 shows that the flaps of the EET configuration (a moderately performing high-lift system by today's standards) are about 5–7% more effective than predicted by the DATCOM method. A second example is the maximum lift prediction for the two-element airfoil in Fig. 4. Here the experimental results indicate an increase in maximum lift coefficient $\Delta C_{l_{max}} = 1.27$ caused by a flap deflection of 20 deg. The computational prediction is close and indicates $\Delta C_{l_{max}} = 1.35$, whereas DATCOM underpredicts the increase and indicates $\Delta C_{l_{max}} = 0.92$. To overcome the limitations of methods such as those found in DATCOM, a new methodology for conceptual high-lift system design has been developed.

One key element of the methodology is called the level 1 aerodynamic database (Fig. 2). This is an extensible database containing two-dimensional geometric and aerodynamic performance data for a variety of high-lift systems. From the information in this database, semi-empirical relationships used for two-dimensional aerodynamic performance prediction of high-lift systems are developed and updated. The resulting high-lift predictive capabilities are well suited for the conceptual design stage of modern civil transport aircraft because the method reflects the current state of high-lift technology and provides fast predictions based on data attained at flight Reynolds numbers.

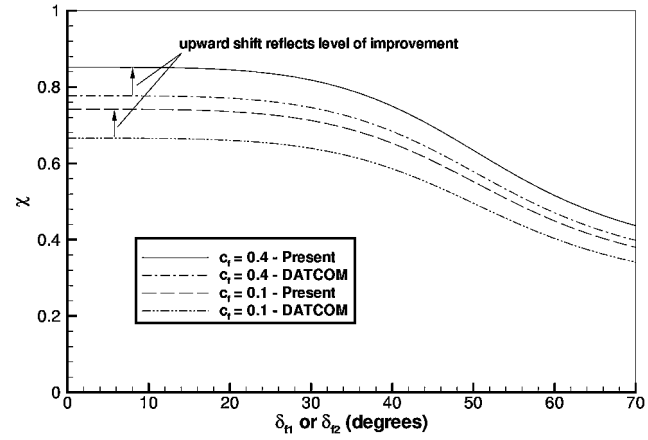

Fig. 6 Comparison of DATCOM[21] and present methodology for flow separation factor for slotted flaps.

The complexity of developing semi-empirical performance prediction relationships was mitigated by assuming no coupling of aerodynamic effects between the leading- and trailing- edge devices. In many cases this decoupled treatment of the problem gives good results, but as Woodward and Lean[10] show the interactive effect of leading- and trailing-edge devices can at times be significant. As more multielement high-lift data become available and we begin to better understand the interaction between the various elements, the level 1 database can be expanded, and the semi-empirical relationships updated to account for the interaction between high-lift airfoil elements.

The two-dimensional level 1 methods are most useful at the conceptual design stage when the information available on the high-lift system is limited to several key design parameters, namely the chord length of each of the elements, trailing- and leading-edge deflection angles, shroud lengths, and airfoil sectional thickness. These parameters along with the aerodynamic characteristics of the clean (cruise) airfoil are required to compute the aerodynamic moments and forces of the high- lift airfoil.

A database for single-slotted trailing-edge and a variety of leading-edge devices was developed previously, and the resulting semi-empirical relationships are presented by Pepper et al.[5] and Pepper and van Dam.[6] More recently, these semi-empirical relationships were extended to include two-dimensional aerodynamic prediction capabilities for main/aft double-slotted trailing-edge devices.[23]

Three-Dimensional Aerodynamic Modeling

A modified lifting-line method based on theory originally developed by Mutterperl[24] and Weissinger[25] and later simplified by Campbell[26] and Blackwell[27] is used to compute the load distribution in subsonic compressible flow of arbitrary wings and lifting surface arrangements. The simplification involves replacing the continuous lifting line of varying strength by a discrete system of horseshoe vortices, each of which is of constant strength. The resulting method, called *finite-step method* or *vortex step method*,[28] allows one to couple sectional (two-dimensional) viscous results with inviscid wing (three-dimensional) theory in order to determine the total aerodynamic coefficients for configurations including wings with dihedral, endplates/winglets, pylons, and biplanes, joined wings, etc. The present method has advantages over the traditional panel or vortex lattice methods because this method is significantly faster than traditional panel methods, and it also incorporates the critical viscous nature of high-lift devices.

The modified Weissinger method used in the high-lift module is discussed in more detail by Paris[23] and Vander Kam.[29] This method represents the lifting surfaces by a system of rectangular horseshoe vortices placed along the quarter-chordline of the lifting surfaces as illustrated in Fig. 7. The load distribution is calculated by solving a linear system of equations that enforce a flow tangency condition at the specified control points. For subsonic flow the effects of Mach number on lift-curve slope and control point position are taken into account using the Prandtl–Glauert equation. The lift is integrated directly from the calculated load distribution. The induced drag is calculated based on the velocities in the Trefftz plane. If the profile drag of the individual airfoil sections is available, it can be integrated along the span of the wing and added to the induced drag to get the total drag of the configuration. The total pitching moment is calculated by translating the sectional pitching moment to a wing reference line and integrating along the span of the wing.

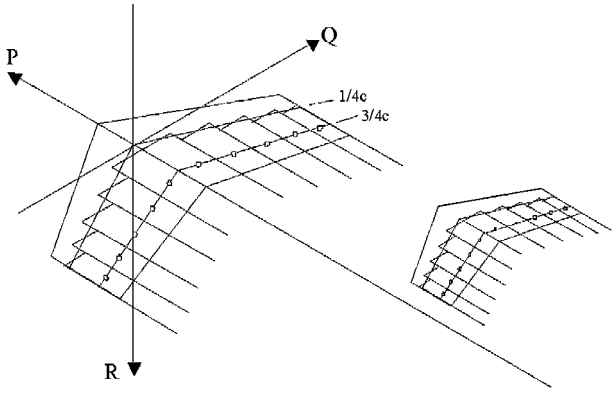

Fig. 7 Distribution of horseshoe vortices over a multiple lifting-surface configuration.[27]

Although the modified Weissinger method reduces the lifting surfaces to flat plates, various airfoil shapes, including high-lift configurations, can be successfully modeled. This is done by adjusting the location of the control points to reflect the proper lift-curve slope and the panel incidence angles to reflect the zero-lift angle of attack of the airfoil. Using this methodology, a variety of test cases have been analyzed to validate the three-dimensional portion of the high-lift module. These test cases will be discussed in the sections to follow.

The modified Weissinger method is capable of analyzing complete aircraft lifting surface configurations, including the main wing with high-lift system, horizontal tail and/or canard, and vertical tail. The geometry of these surfaces can include sweep, taper, twist, and dihedral. Additional features that have been added to the three-dimensional portion of the high-lift module include a simple fuselage model, a nonlinear $C_{L_{\max}}$ prediction routine, and a wind-tunnel wall model. The $C_{L_{\max}}$ prediction routine is discussed in the next section, whereas more information regarding the fuselage and wind-tunnel wall models can be found in the report by Paris.[23]

Maximum Lift Prediction

The nonlinear method for predicting $C_{L_{\max}}$ couples the modified Weissinger method with two-dimensional viscous flow calculations (or experimental data). At a minimum two-dimensional lift data are required for the wing root and wing tip sections. If there exists a significant variation in the spanwise airfoil geometry, such as the case of high-lift configurations and most cruise wings, sectional data for additional stations along the wing should be used. INS2D has shown much promise in its ability to accurately predict two-dimensional viscous flows for both single- and multielement airfoils. Considerable success has been achieved using the Spalart–Allmaras turbulence model[15] and by exercising special care in the specification or prediction of boundary-layer transition locations.

The lift data for each defining airfoil section are compiled into a single data file that is read by the high-lift module. The lift-curve slope C_{l_α} and zero-lift angle of attack α_0 are then calculated for each section. This information is used in the present method to calculate the initial load distribution from which the local coefficient of lift is calculated for each spanwise station. After this initial three-dimensional calculation the following iterative procedure is performed for each angle of attack being examined:

1) Calculate the effective local angle of attack for each station using:

$$\alpha_{\text{local}} = C_{l_w}/C_{l_\alpha} + \alpha_0 - \Delta\alpha_{\text{visc}}$$

where the local lift coefficient C_{l_w} is calculated for each station from the bound vortex strength and $\Delta\alpha_{\text{visc}}$ is the viscous correction angle (see step 3), which is initially equal to zero.

2) Find $C_{l_{\text{visc}}}$ at the local angle of attack α_{local} by interpolating the two-dimensional viscous section input data.

3) If $|C_{l_{\text{visc}}} - C_{l_w}| > \varepsilon$, with a typical value for $\varepsilon = 0.01$, determine the appropriate viscous correction angle for each section such that at the local angle of attack the lift coefficient of the corrected section equals $C_{l_{\text{visc}}}$ using the following:

$$\Delta\alpha_{\text{visc}} = (C_{l_{\text{visc}}} - C_{l_w})/C_{l_\alpha}$$

See Fig. 8 for a graphical description of $\Delta\alpha_{\text{visc}}$.

4) Adjust the α distribution (left-hand side of system of equations in the modified Weissinger method) by the appropriate local viscous correction angle $\Delta\alpha_{\text{visc}}$, and calculate the resulting load distribution.

5) Repeat steps 1–4 until $|C_{l_{\text{visc}}} - C_{l_w}| < \varepsilon$ for all spanwise stations.

This iterative procedure is performed for a complete angle-of-attack sweep. The maximum lift coefficient and stall angle can easily be determined from the resultant lift curve. This iterative procedure has proven to be robust even when encountering negative sectional lift-curve slopes at poststall conditions. However, as pointed out by Kroeger and Feistel[30] care should be taken in applying nonlinear lifting-line methods to poststall calculations. Several validation test cases used in the validation of the $C_{L_{\max}}$ prediction routine are presented and discussed next.

Results and Discussion

Five test cases are presented that depict the capabilities and accuracy of the hybrid flow solution method and in particular the $C_{L_{\max}}$ prediction routine. These test cases are as follows: 1) F-29, cruise configuration, which demonstrates accuracy of $C_{L_{\max}}$ prediction routine for a cruise configuration; 2) flapped half-span wing, full-span flaps, which demonstrate accuracy of $C_{L_{\max}}$ prediction routine for a high-lift configuration and validate wind-tunnel wall model in high-lift module; 3) flapped half-span wing, part-span flaps, which demonstrate importance of nonplanar wake effect and validate modified trailing-wake model; 4) close-coupled canard, which validates multiple lifting surface predictions; and 5) RAE 1372, clean, full and partial-span flaps, which demonstrate accuracy of lift prediction for typical high-lift configuration.

The first test case is of the F-29 swept cruise wing configuration shown in Fig. 9 (Ref. 31). The wing has 21 deg of sweep at the quarter-chord, aspect ratio 10, and taper ratio 0.23. The high-lift module utilized two-dimensional aerodynamic data at nine different spanwise locations, as indicated in Fig. 9, for the nonlinear $C_{L_{\max}}$ calculations. The correlation with experimental data is excellent and can be seen in Fig. 10. The good agreement between the experimental data and the present prediction demonstrates that the nonlinear $C_{L_{\max}}$ prediction routine works very well for cruise wing configurations, provided accurate two-dimensional sectional data are available.

The next high-lift test case was chosen as an example application of the wind-tunnel wall correction capabilities and also to further validate the method. The configuration selected was a wing with no sweep or taper having $AR = 5.9$ and NACA 0012 airfoil sections.[32,33] The half-span wing model, shown in Fig. 11, was tested in the Langley 14×22 Ft subsonic wind tunnel, and the data reported had no wind-tunnel wall corrections applied. The lift curves for the full-span flapped high-lift test case, as shown in Fig. 12, demonstrate that the vortex image method for modeling wind-tunnel walls does indeed provide accurate predictions in lift. In addition, Fig. 12 shows that the nonlinear $C_{L_{\max}}$ prediction routine continues to accurately predict the stall angle and maximum lift of the high-lift wing.

The half-span NACA 0012 wing from the preceding test case was also analyzed in the part-span flap configuration (test case 3). As in the full-span flapped case, the results verify that the wind-tunnel modeling method used in the high-lift module does indeed provide results consistent with test data. The lift curves presented in Fig. 13 show that with the wind-tunnel wall corrections inactive, the lift-curve slope predicted by the high-lift module is less than the experimental lift-curve slope. Turning the wind-tunnel wall model on brings the high-lift module lift prediction into agreement with the experimental data.

Unexpectedly, the prediction of $C_{L_{\max}}$ for the part-span test case was much lower than the experimentally determined value as shown

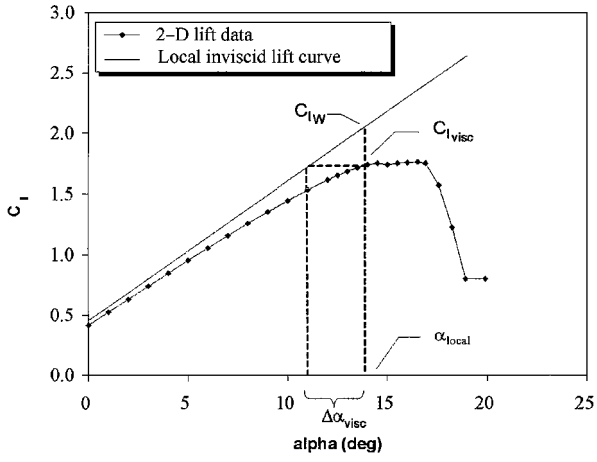

Fig. 8 Definition of viscous correction angle as part of nonlinear $C_{L_{\max}}$ prediction routine.

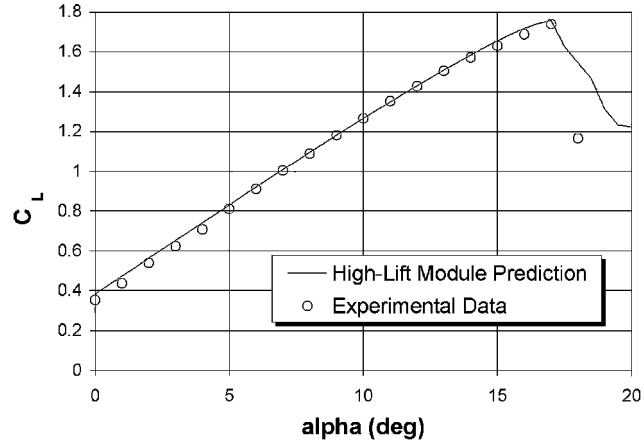

Fig. 10 Comparison of predicted and measured lift curves for wing-body configuration at $M_\infty = 0.19$, $Re_{MAC} = 5.0 \times 10^6$.

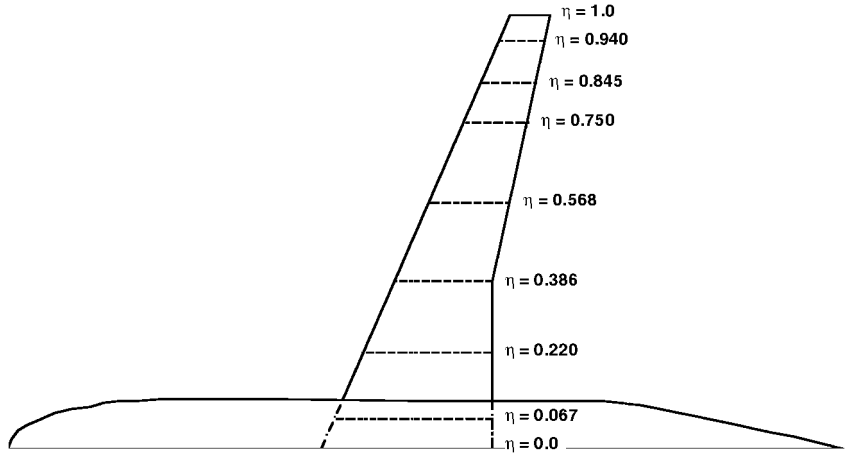

Fig. 9 Wing-body configuration with two-dimensional aerodynamic data specified at nine stations indicated.[31]

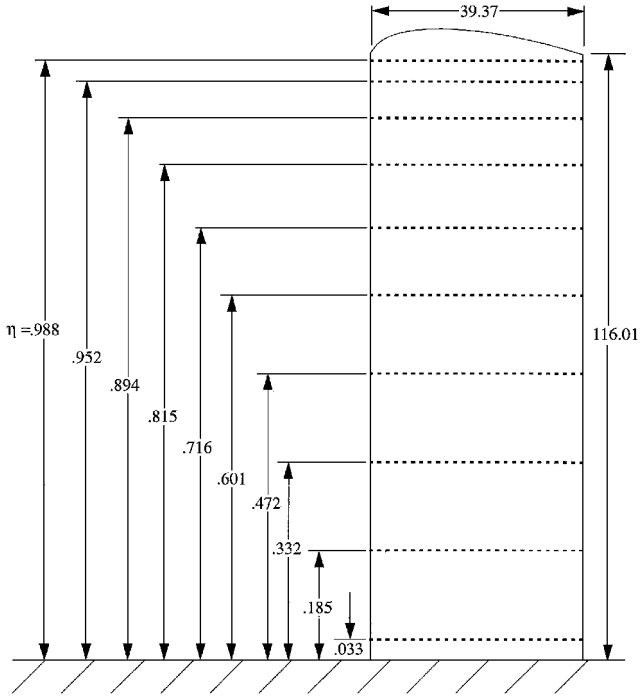

Fig. 11 Geometry description and pressure tap locations of NACA 0012 semispan test case.[32]

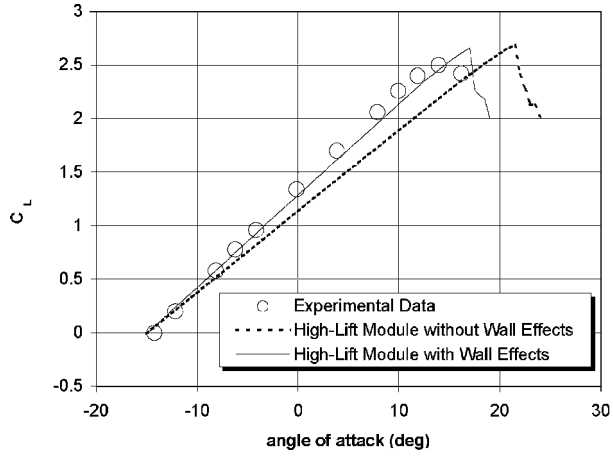

Fig. 12 Lift curves with and without wind-tunnel wall effect for NACA 0012 full-span flap test case at $M_\infty = 0.15$, $Re = 3.3 \times 10^6$.

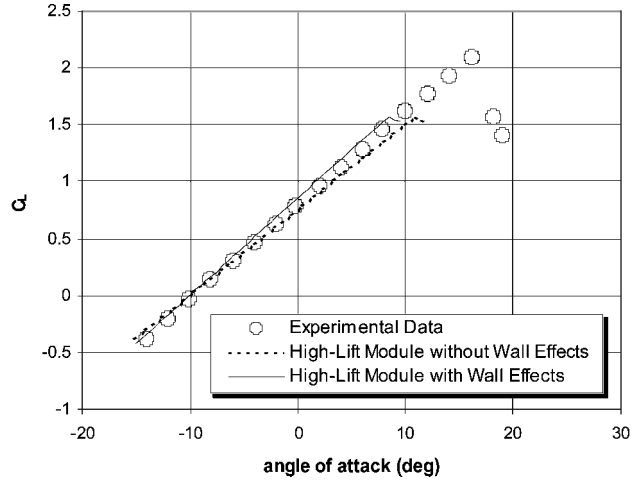

Fig. 13 Lift curves with and without wind-tunnel wall effect for NACA 0012 partial-span flap test case at $M_\infty = 0.15$, $Re = 3.3 \times 10^6$ (modified Weissinger method with planar wake).

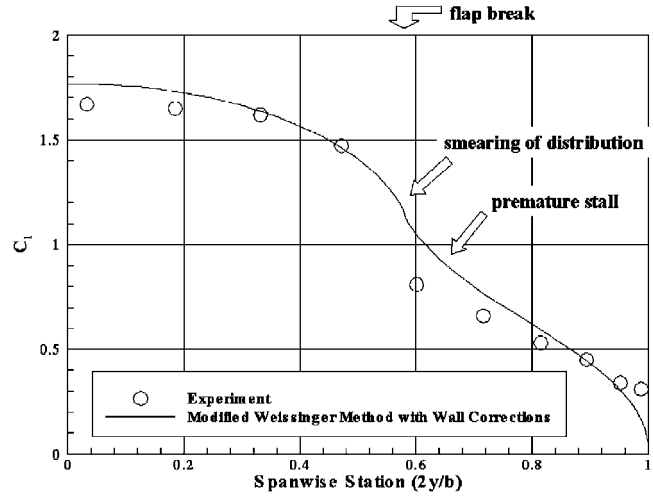

Fig. 14 Spanwise load distribution for NACA 0012 partial-span flap test case at $\alpha = 4$ deg (modified Weissinger method with planar wake).

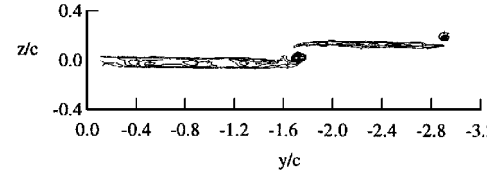

Fig. 15 Wake contours (total pressure) measured at 0.1*c* aft of flap trailing edge of NACA 0012 partial-span flap wing at $\alpha = 4$ deg.[34]

in Fig. 13. Up to this point, the nonlinear $C_{L\max}$ prediction method had produced results very consistent with experiment. After further investigation it was discovered that this discrepancy in test case 3 arises from a smearing of the spanwise load distribution that occurs at the flap break (or other discrete change in geometry such as a thrust gate) and is a result of the simplifying assumptions of the modified Weissinger method. The smearing effect occurs because the planar wake assumption tends to cause an overshoot in the effective angle of attack on either side of the flap break. This results in an artificially increased loading of the unflapped region, thus causing a premature stall of the unflapped region. This effect is exhibited in the spanwise load distribution for test case 3, as shown in Fig. 14.

The smearing in the load distribution is believed to occur because the modified Weissinger method models the trailing vortex wake in a single plane. Experimental and computation results indicate that the wake is not planar, but rather has discrete jumps where geometric discontinuities exist in the lifting surface. Figure 15 illustrates this nonplanar wake development behind the part-span high-lift wing. This picture illustrates that the trailing vortical wake just downstream of the flapped region is in a completely separate plane from the vortical trailing wake of the unflapped region.

It became evident that a different method, one that allows for nonplanar wake modeling, is required to accurately predict the three-dimensional aerodynamic characteristics of high-lift wings. After implementing a nonplanar wake model in the Weissinger code, the spanwise load distribution depicts the steep drop at the flap break (Fig. 16). Also, the maximum lift prediction is much improved and much better agreement with the experimental results is obtained as shown in Fig. 17. Details of the nonplanar wake formulation may be found in the report by Vander Kam.[29] Wakayama and Kroo[35] do not model the nonplanar wake effect but instead include a semi-empirical function that modifies the induced velocities and sectional maximum lift coefficients in the flap-edge region based on the hypothesis that the vortex system originating at the flap edge modifies the effective sectional camber.

The fourth test case was selected in order to validate the capabilities of the method for configurations containing multiple lifting surfaces. In this configuration two rectangular planforms utilizing

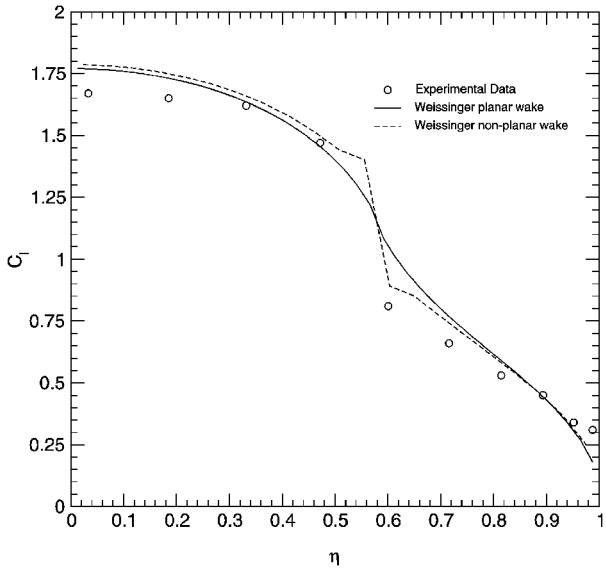

Fig. 16 Predicted spanwise load distribution for NACA 0012 partial-span flap test case at $\alpha = 4$ deg.

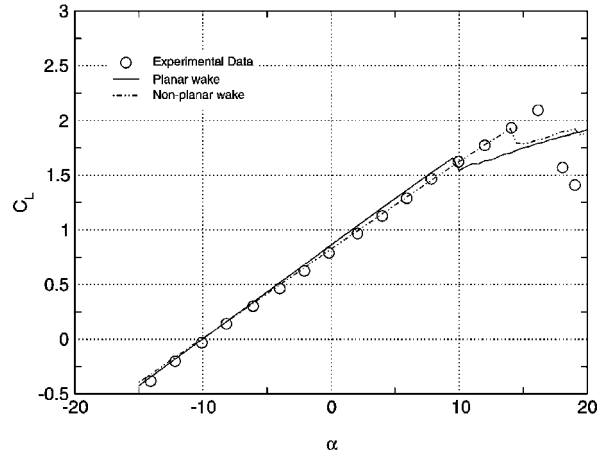

Fig. 17 Lift curves with wind-tunnel wall effect for NACA 0012 partial-span flap test case at $M_\infty = 0.15$, $Re = 3.3 \times 10^6$.

the LS(1)-0413 airfoil section make up a wing-canard configuration as seen in Fig. 18 (Ref. 36). This configuration was tested at the NASA Ames 7 × 10 ft tunnel. In the arrangement discussed here the wing and canard are 0.48 m ($1.6c_{\text{wing}}$) apart horizontally and the wing is 0.15 m ($0.5c_{\text{wing}}$) below the canard. Two-dimensional sectional data were obtained using INS2D and the aforementioned transition prediction algorithm. Lift and moment results are shown in Figs. 19 and 20, respectively. These results demonstrate the accuracy of the method for multiple lifting surface configurations.

The final test case is that of the RAE 1372 tested at the No. 2 $11\frac{1}{2} \times 8\frac{1}{2}$ ft tunnel at Farnborough, England.[37] This configuration consists of a swept wing evaluated in the clean configuration as well as with full and 80% span flaps deflected 10 and 25 deg. The wing sweep angle is 28 deg at the quarter-chord, the aspect ratio is 8.35, and the taper ratio is 0.35. The configuration is depicted in Fig. 21. Again, two-dimensional sectional data were obtained using INS2D and the transition prediction method already discussed. The flap coordinates provided in the experimental report were quite coarse and required that the leading-edge region be refined with a cubic spline. This refinement introduces some uncertainty into the two-dimensional predictions as the proper geometry is unknown in this critical area of the airfoil.

Figure 22 illustrates the accuracy of lift predictions for the clean configuration. Figure 23 presents lift results for the full-span flap case, and Fig. 24 presents lift results for the 80% span flap case. There is some discrepancy in the results for the 25-deg flaps setting,

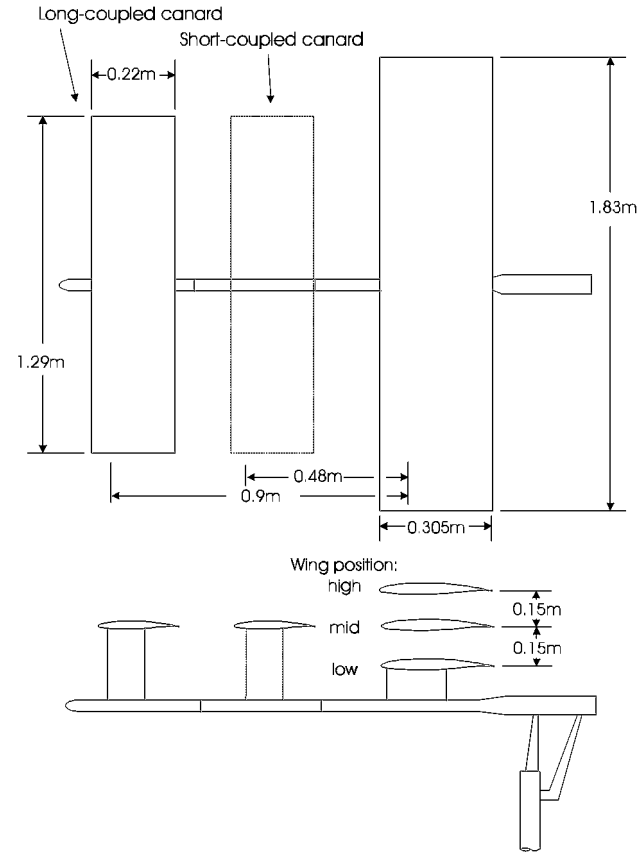

Fig. 18 Geometry definition of the canard test case.[36]

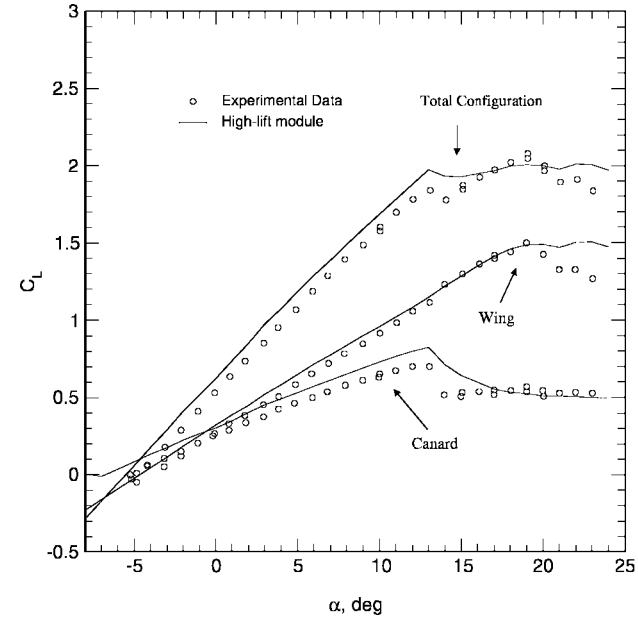

Fig. 19 Lift results for the close-coupled wing-low canard test case, $Re = 1.4 \times 10^6$.

which can be caused by the aforementioned flap coordinate issue. The proper amount of required geometry refinement was not known and may not reflect the actual test case geometry to within a negligible margin of error. Nonetheless, these results illustrate that the method is capable of highly accurate results for realistic geometries in the clean and high-lift configurations.

In summary, the flow solver that is part of the high-lift module produces excellent results for cruise and high-lift wings including wings with partial-span flaps. In addition, the wind-tunnel wall

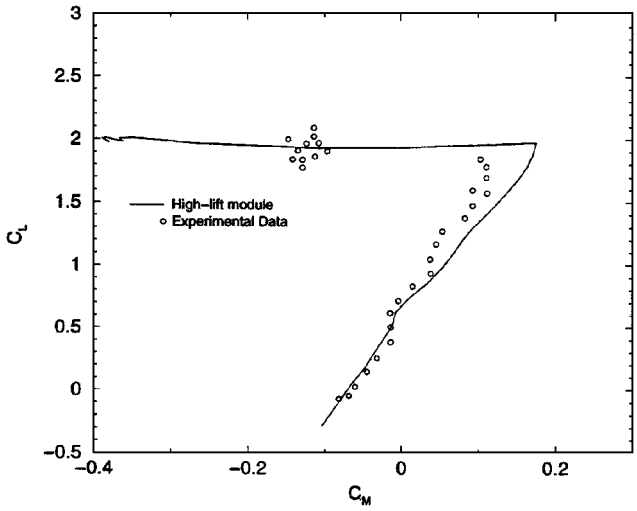

Fig. 20 Pitching moment results for the close coupled wing-low canard test case, $Re = 1.4 \times 10^6$.

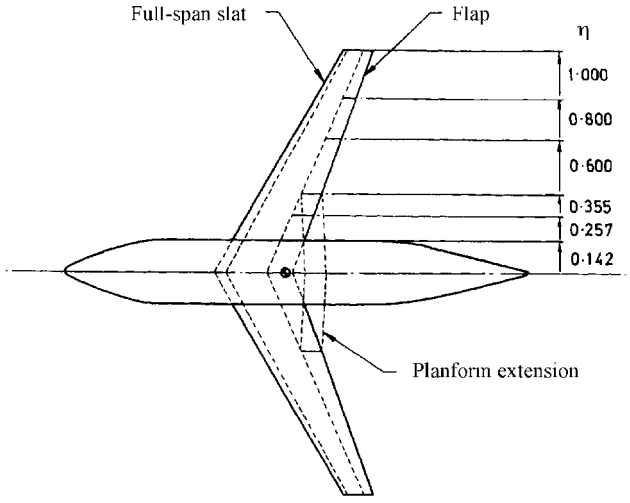

Fig. 21 RAE 1372 geometry definition.[37]

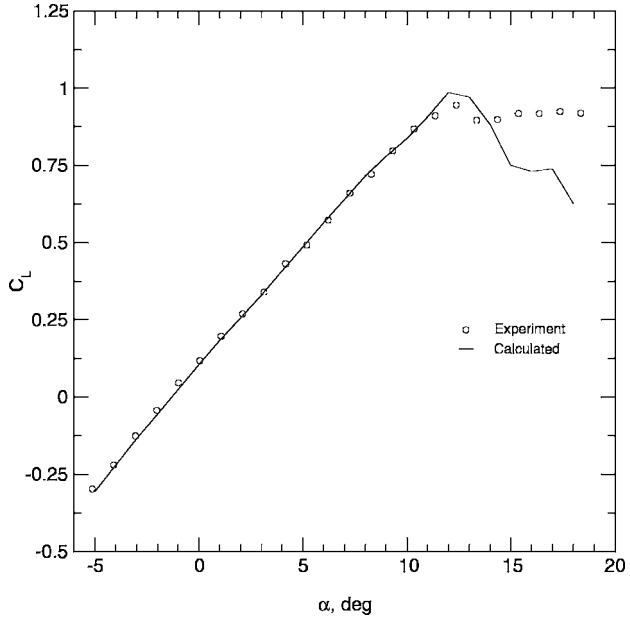

Fig. 22 Lift results for the clean RAE 1372 configuration, $Re = 1.35 \times 10^6$, $M_\infty = 0.233$.

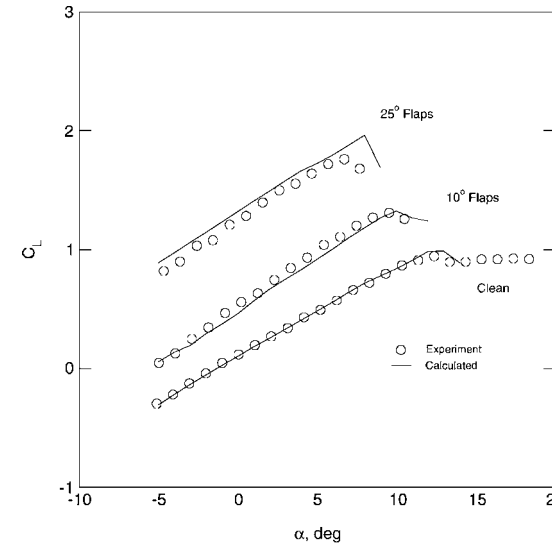

Fig. 23 Effect of full-span flaps on the RAE 1372 test case, $Re = 1.35 \times 10^6$, $M_\infty = 0.233$.

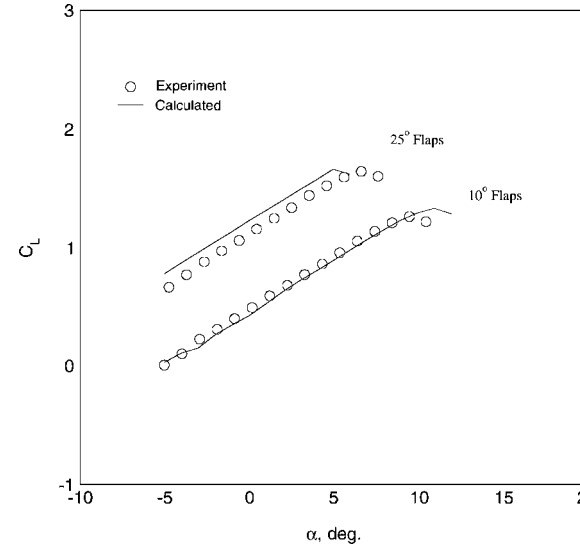

Fig. 24 Effect of 80% span flaps on the RAE 1372 test case, $Re = 1.35 \times 10^6$, $M_\infty = 0.233$.

model and fuselage models are working quite well. It provides an excellent compromise between computing time and accuracy for calculating the high-lift performance of an aircraft at the conceptual and preliminary design stages.

Conclusions

The highly competitive and economically driven commercial aviation market of today requires that aircraft manufacturers be able to provide customers with a high-quality product within the shortest amount of time at the lowest possible cost. An important key to reducing both the investment and operating cost of an aircraft is to keep the systems as simple as possible. At one point in history, the complexity of high-lift systems was gradually increasing in order to achieve higher aerodynamic performance, but recent trends are headed in the opposite direction and aircraft companies are designing high-lift systems that achieve given levels of lift with simpler systems. To facilitate the efforts to design simpler, and thus more cost-effective high-lift systems, the present high-lift design methodology has been developed to offer significant improvements over traditional methods.

Noting the importance of designing simpler high-lift systems, it is critical that high-lift system considerations be included at even

the earliest stages of the design process. In response to this need, a high-lift system design methodology has been developed that can be effectively utilized in both the conceptual and preliminary design stages of an aircraft. This makes it possible for the designer or aircraft optimization package to examine, early on in the design process, the effects that various high-lift configurations have on the overall cost and performance of a transport aircraft.

For a design tool be to effective at the conceptual and preliminary design stages, it must provide a reasonable balance between speed and accuracy. Keeping this in mind, a fast modified Weissinger method was chosen for the three-dimensional aerodynamic analysis. The three-dimensional calculations are coupled with two-dimensional viscous data, which enable the method to produce good results at a fraction of the time required for three-dimensional Navier–Stokes solutions. The test cases and sample application presented in this report demonstrate that this method does indeed provide the necessary accuracy to be useful at the conceptual and preliminary design stages, while being fast enough to be used during the early stages of design where thousands of iterations can be examined.

The methodology presented in this report has been integrated into an existing high-lift system design computer code, referred to as the "high-lift module." This high-lift module is simple to use and is capable of analyzing a wide range of high-lift systems found on general aviation and civil transport aircraft.

Acknowledgments

This work has been supported by the NASA Ames Research Center, Moffet Field, CA, under Consortium Agreements NCC2-5188 and NCC2-5255 and by the NASA Langley Research Center, Hampton, VA, under Grant NAG-1-2215. We also would like to acknowledge the contributions and feedback provided by Paul Gelhausen, NASA Langley Research Center; David Kinney, NASA Ames Research Center; Mark Waters, Eloret, Inc., and Nico Vougt, The Boeing Company.

References

[1]Rudolph, P. K. C., "High-Lift Systems on Commercial Subsonic Airliners," NASA CR 4746, Sept. 1996.

[2]Nield, B. N., "An Overview of the Boeing 777 High-Lift Aerodynamic Design," *Aeronautical Journal*, Vol. 99, No. 989, 1995, pp. 361–371.

[3]Davis, P., "Industrial Strength Optimization at Boeing," *SIAM News*, Vol. 29, No. 1, 1996.

[4]Myklebust, A., and Gelhausen, P., "Putting the ACSYNT on Aircraft Design," *Aerospace America*, Vol. 32, No. 9, 1994, pp. 26–30.

[5]Pepper, R. S., van Dam, C. P., and Gelhausen, P. A., "Design Methodology for High-Lift Systems on Subsonic Aircraft," AIAA Paper 96-4056, Sept. 1996.

[6]Pepper, R. S., and van Dam, C. P., "Design Methodology for High-Lift Systems on Subsonic Civil Transport Aircraft," NASA CR 202365, Aug. 1996.

[7]van Dam, C. P., Shaw, S. G., Vander Kam, J. C., Brodeur, R. R., Rudolph, P. K. C., and Kinney, D., "Aero-Mechanical Design Methodology for Subsonic Civil Transport High-Lift Systems," *Aerodynamic Design and Optimisation of Flight Vehicles in a Concurrent Multi-Disciplinary Environment*, NATO Research and Technology Organization, RTO MP 35, 2000, pp. 7-1–7-12.

[8]van Dam, C. P., Shaw, S. G., Vander Kam, J. C., Rudolph, P. K. C., and Kinney, D., "Aero-Mechanical Design of High-Lift Systems," *Aircraft Engineering and Aerospace Technology*, Vol. 7, No. 5, 1999, pp. 436–443.

[9]Cahill, J. F., "Summary of Section Data on Trailing-Edge High-Lift Devices," NACA Rept. 938, 1949.

[10]Woodward, D. S., and Lean, D. E., "Where Is High-Lift Today?—A Review of Past UK Research Programmes," *High-Lift System Aerodynamics*, AGARD CP-515, 1993, pp. 1-1–1-45.

[11]Rogers, S. E., and Kwak, D., "An Upwind Differencing Scheme for the Incompressible Navier–Stokes Equations," *Applied Numerical Mathematics*, Vol. 8, No. 1, 1991, pp. 43–64.

[12]Rogers, S. E., Wiltberger, N. L., and Kwak, D., "Efficient Simulation of Incompressible Viscous Flow over Single and Multielement Airfoils," *Journal of Aircraft*, Vol. 30, No. 5, 1993, pp. 736–743.

[13]Lin, J. C., and Dominik, C. J., "Parametric Investigation of a High-Lift Airfoil at High Reynolds Numbers," *Journal of Aircraft*, Vol. 34, No. 4, 1997, pp. 485–491.

[14]Eyi, S., Lee, K. D., Rogers, S. E., and Kwak, D., "High-Lift Design Optimization Using Navier–Stokes Equations," *Journal of Aircraft*, Vol. 33, No. 3, 1996, pp. 499–504.

[15]Spalart, P. R., and Allmaras, S. R., "A One-Equation Turbulence Model for Aerodynamic Flows," *La Recherche Aérospatiale*, No. 1, 1994, pp. 5–21.

[16]Rogers, S. E., Menter, F., Durbin, P. A., and Mansour, N. N., "A Comparison of Turbulence Models in Computing Multi-Element Airfoil Flows," AIAA Paper 94-0291, Jan. 1994.

[17]Kusunose, K., and Cao, H. V., "Prediction of Transition Location for a 2-D Navier–Stokes Solver for Multi-Element Airfoil Configurations," AIAA Paper 94-2376, June 1994.

[18]van Dam, C. P., Los, S. M., Miley, S., Roback, V. E., Yip, L. P., Bertelrud, A., and Vijgen, P. M. H. W., "In-Flight Boundary-Layer Measurements on a High-Lift System: Main Element and Flap," *Journal of Aircraft*, Vol. 34, No. 6, 1997, pp. 757–763.

[19]Brodeur, R. R., and van Dam, C. P., "Transition Prediction for a Two-Dimensional Navier–Stokes Solver Applied to Wind-Turbine Airfoils," AIAA Paper 2000-0047, Jan. 2000.

[20]van den Berg, B., "Boundary-Layer Measurements on a Two-Dimensional Wing with Flap," National Aerospace Lab., NLR TR 79009U, the Netherlands, Jan. 1979.

[21]Hoak, D., "USAF DATCOM Section 6—Characteristics of High-Lift and Control Devices," Flight Control Div., Air Force Flight Dynamics Lab., Wright-Patterson, OH, 1974 (revised).

[22]Henderson, M. L., "High Lift Selected Concepts," NASA CR 159093, Aug. 1979.

[23]Paris, J. K., "Advancements in the Design Methodology for Multi-Element High-Lift Systems on Subsonic Civil Transport Aircraft," M.S. Thesis, Dept. of Mechanical and Aeronautical Engineering, Univ. of California, Davis, 1999.

[24]Mutterperl, W., "The Calculation of Span Load Distributions on Swept-Back Wings," NACA TN 834, Dec. 1941.

[25]Weissinger, J., "The Lift Distribution of Swept-Back Wings," NACA TM 1120, March 1947.

[26]Campbell, G. S., "A Finite-Step Method for the Calculation of Span Loadings of Unusual Plan Forms," NACA RM L50L13, 1951.

[27]Blackwell, J. A., "A Finite-Step Method for Calculation of Theoretical Load Distributions for Arbitrary Lifting-Surface Arrangements at Subsonic Speeds," NASA TN D-5335, July 1969.

[28]Barnes, J. P., "Semi-Empirical Vortex Step Method for the Lift and Induced Drag Loading of 2D or 3D Wings," Society of Automotive Engineers, SAE Paper 975559, Oct. 1997.

[29]Vander Kam, J. C., "Reduced-Order High-Fidelity Methodologies for the Design of Civil Transport High-Lift Systems," M.S. Thesis, Dept. of Mechanical and Aeronautical Engineering, Univ. of California, Davis, July 2000.

[30]Kroeger, R. A., and Feistel, T. W., "Reduction of Stall-Spin Entry Tendencies Through Wing Aerodynamic Design," Society of Automotive Engineers, Paper 760481, April 1976.

[31]Obert, E., "Forty Years of High-Lift R&D—An Aircraft Manufacturer's Experience," *High-Lift System Aerodynamics*, AGARD CP-515, 1993, pp. 27-1, 27-2.

[32]Weston, R. P., "Refinement of a Method for Determining the Induced and Profile Drag of a Finite Wing from Detailed Wake Measurements," Ph.D. Dissertation, Univ. of Florida, Gainesville, 1981.

[33]Applin, Z. T., "Pressure Distributions from Subsonic Tests of a NACA 0012 Semispan Wing Model," NASA TM 110148, Sept. 1995.

[34]Jones, K. M., Biedron, R. T., and Whitlock, M., "Application of a Navier–Stokes Solver to the Analysis of Multielement Airfoils and Wings Using Multizonal Grid Techniques," AIAA Paper 95-1855, June 1995.

[35]Wakayama, S., and Kroo, I., "Subsonic Wing Planform Design Using Multidisciplinary Optimization," *Journal of Aircraft*, Vol. 32, No. 4, 1995, pp. 746–753.

[36]Feistel, T. W., Corsiglia, V. R., and Levin, D. B., "Wind-Tunnel Measurements of Wing-Canard Interference and a Comparison with Various Theories," Society of Automotive Engineers, SAE Paper 810575, April 1981.

[37]Lovell, D. A., "A Wind-Tunnel Investigation of the Effects of Flap Span and Deflection Angle, Wing Planform and a Body on the High-Lift Performance of a 28° Swept Wing," Aeronautical Research Council, ARC C.P. 1372, U.K., 1947.